

30 Mar 2001, 1:30 pm - 3:30 pm

# Identification of Different Seismic Waves Generated by Foundation Vibration in the Centrifuge: Travel Time, Spectral and Numerical Investigations

Jean-Louis Chazelas
*Laboratoire Central des Ponts et Chaussées, France*

Odile Abraham
*Laboratoire Central des Ponts et Chaussées, France*

Jean-François Semblat
*Laboratoire Central des Ponts et Chaussées, France*

**Proceedings: Fourth International Conference on Recent Advances in Geotechnical Earthquake Engineering and Soil Dynamics and Symposium in Honor of Professor W.D. Liam Finn**
**San Diego, California, March 26-31, 2001**

# IDENTIFICATION OF DIFFERENT SEISMIC WAVES GENERATED BY FOUNDATION VIBRATION IN THE CENTRIFUGE: TRAVEL TIME, SPECTRAL AND NUMERICAL INVESTIGATIONS

**Jean-Louis Chazelas**
Laboratoire Central des Ponts et Chaussées
BP 4329, 44341 Bouguenais cedex, France

**Odile Abraham**
Laboratoire Central des Ponts et Chaussées
BP 4329, 44341 Bouguenais cedex, France

**Jean-François Semblat**
Laboratoire Central des Ponts et Chaussées
58, boulevard Lefebvre - 75732 Paris cedex 15, France

## ABSTRACT

For the analysis of footings under dynamic loading scaled modeling in the centrifuge assumes that the soil behaves like at prototype scale. This paper demonstrates that for a container filled with dry sand, wave velocities can be described by a model based on the relation between the shear modulus and the depth dependent stress level proposed by Iwasaki and Tatsuoka. A preliminary estimation of the shear wave velocities and of the Poisson's ratio confirms by dynamical measurements the currently use value of 0.25. A FEM modeling also helps to strengthen the validity of the model proposed, providing another insight in the propagation of waves in a soil with a velocity gradient.

## 1 INTRODUCTION

Physical modeling is a powerful mean for analysing the behavior of geotechnical works or for testing numerical models. Scaled modeling in the centrifuge is one of those tools which main force comes from the ability it offers to realize cheap parametric studies. However, it is important to face the fundamental question: are field conditions correctly reproduced ? Another question, linked to the previous one, arises from this modeling: in the case of dynamic soil-structure interaction studies in the centrifuge, how one can cope with the finite dimensions of the soil model ? At prototype scale, the energy radiated by the footings of the tested structures propagates to infinity. In the centrifuge, it is quickly reflected back.

Coe et al. (1985) carried out such tests and demonstrated that the velocity of body waves was proportional to the square root of the stress level induced by the gravity level. Siemer and Jessberger (1994) studied the vertical profile of P-waves velocities using a series of accelerometers embedded vertically under a footing . They showed that it was possible to fit a law of the form proposed by Iwasaki and Tatsuoka (1977) linking the dynamic shear modulus Gmax to the mean stress in the soil. Kita et al. (1992) established the same kind of relation at different gravity levels using a piezoelectric device able to generate S-waves directly in the sand. In another direction, Semblat and Luong (1998) made an extended study principally aimed at characterizing the damping of waves in the sand of the container. This paper intends to completes these findings by an overview of wave propagation characteristics in the whole. An analysis of the wave field generated in the container by surface footings loaded with a vertical impact is presented. This kind of load has been chosen because, along with a high-frequency acquisition, it provides a possibility to observe the arrival of waves at different locations of the container and a mean to study impedance functions (see Paper 9.35). P-wave velocities will be examined vertically under the footing and horizontally near the surface. They will be related to the dynamic shear modulys and its known dependency on the stress level. The shear wave velocities and the Poisson's ratio will be estimated implementing the SASW (Spectral Analysis of Surface Waves) under simplified but validated assumptions. FEM modeling of the propagation in the container gives another insight into propagation phenomena : the localization and the relative importance of P-waves and Rayleigh waves.

## 2 TESTING PROGRAM

### Experimental setup

The series of tests have been carried out on the 200 g-ton centrifuge of the Laboratoire Central des Ponts et Chaussées– France. Large rectangular 1.20 x 0.80 x 0.36 m containers were used. In order to show the influence of both impact loading and boundary lining, two containers have been tested: one without and one with a 2.5 cm Duxseal coating, the density of sand being kept, theoretically, the same. The model soil was a fine dry Fontainebleau sand, rained into the container for a density of 16.30 kN/m$^3$ ($I_D$=0.79).

The model footings were aluminum cylinders or square plates lying on the sand (see table I). The hammer was a seesaw supported by a beam over the container with a PCB 200A2 force transducer at one end and an electromagnetic jack at the other end, driven from the command room.

Table I Characteristics of the footings under test

| Circular footings | | | | Square footings | | | |
|---|---|---|---|---|---|---|---|
| # | mass kg | ∅ mm | prototype mass /50 g | # | Mass Kg | Dim. mm | prototype mass /50 g |
| 1 | 0.118 | 60 | 14.3 T | 5 | 0.046 | 26x26 | 5.7 T |
| 2 | 0.237 | 60 | 28.6 T | 6 | 0.200 | 52x52 | 23.7 T |
| 3 | 0.129 | 50 | 16,6 T | | | | |

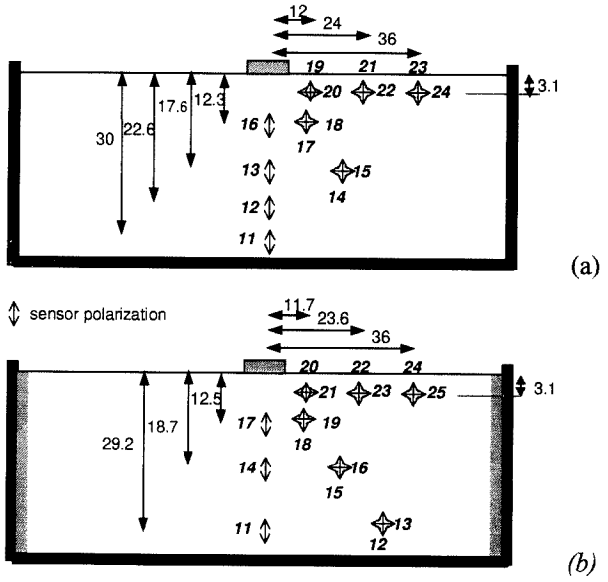


*Fig. 1: Location and direction of the accelerometers in the sand (a: container without Duxseal – b: container with Duxseal) - dimensions in cm.*

PCB 352A10 accelerometers were embedded in the sand at different locations (see Fig.1) in order to register local acceleration amplitudes and wave directions. As the tests were carried out at 30, 40 and 50 g, we had a full insight of stress influence: as well as depth and gravity level. Each trail was repeated five time in order to enable stacking of data.

Output data were amplified in the basket and digitized with a device at the centrifuge pivot before transfer to the computer via the slip rings. All data treatments have been post processed.

## EXPERIMENTAL RESULTS

### P-Wave Velocities

Mean velocities of P-waves were firstly estimated using the first arrival on accelerometers placed on a vertical line under the footings. For a comparison of results from different gravity levels, the velocities are plotted in Fig.2 *vs.* the produce g.z of the gravity and the depth. According to the aforementioned works, these velocities are increasing with depth as well as the gravity level. Iwasaki and Tatsuoka (1977) established that:

$$Gmax = 9.10^5.\frac{(2.17-e)^2}{1+e}.\sigma_o^{0.4} \quad (1)$$

where e is the void ratio and $\sigma_o$ the mean stress. Along with the classical relations:

$$Vp = \sqrt{\frac{2.(1-\nu)}{1-2.\nu}}.\sqrt{\frac{G}{\rho}} \quad \text{and} \quad \sigma_o = \frac{1}{3}.\frac{1+\nu}{1-\nu}.\rho.g.z \quad (2)$$

we should find a relation of the form: $Vp = k.(g.z)^{0.2}$ (3)

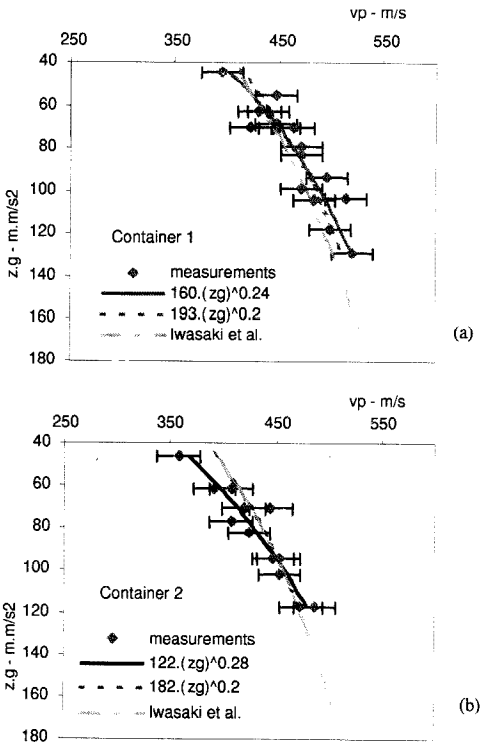


*Figure 2 : P-wave velocities vs. depth under the source*

Both graphs show a rather good agreement of measured data with a fitted curve corresponding to equation (3) (in dotted line), but freeing the exponent in the correlation gives a slightly higher value for it (in solid line). However, the number of sensors is limited and the curves stay in the range of the estimated error bars (about 7%). Last, it can be noticed that adopting Iwasaki and Tatsuoka formula (in dashed gray line) is also in good agreement with data.

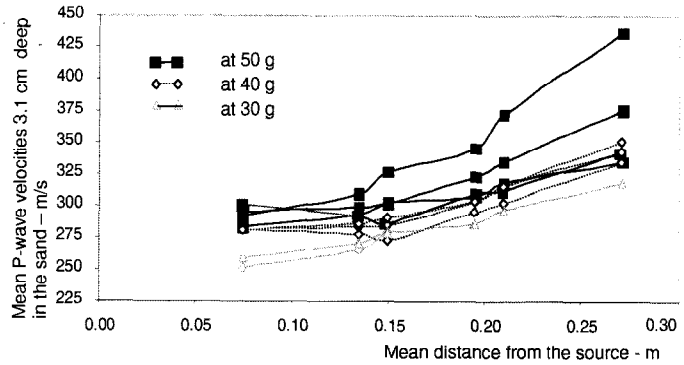


*Fig. 3: Evolution of apparent mean velocities of P-waves near the surface*

Figure 3 shows an amazing result; mean velocities of P-waves, determined as above for sensors placed horizontally 3.1 cm below the surface, seem to increase with distance to footings.

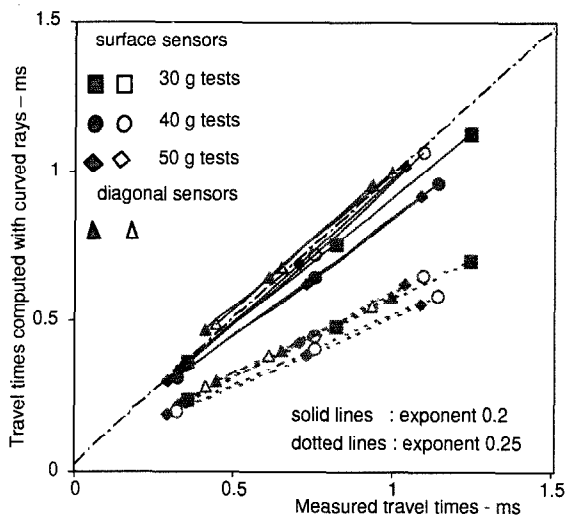


*Fig. 4 : Relation between measured arrival times and computed arrival times on accelerometers embedded below the surface – Curved rays computation.*

The above observed gradient of P-wave velocities leads to assume that rays are curved: the minimum travel time is not the straight line. Thus a simplified model of circular rays has been tested: for each sensor location, the minimal circular travel time has been estimated by integration of local velocities using equations (1) and (2). The source location was supposed to be the point of the footing edge nearest to the sensor. Figure 4 shows a good agreement between the measured travel times and the computed ones for different tests at different gravity levels with curved rays assumption. Moreover, the same computation was applied to sensors placed on a diagonal line under the source (# 18,15 and 12 on Fig.1 b). The result is consistent with those of the other locations. Fig. 4 also shows that the computation with an exponent equal to 0.5 in Iwasaki and Tatsuoka equation is worst unlike that proposed by Hardin and Drnevitch's (1972) and unlike the correlations in Fig. 2 would suggest.

This second result strengthens the validity of the model described by equations (1) and (2).

## S-Waves Velocities

The use of surface waves to determine shear wave velocity profiles is becoming more and more widespread is the civil engineering community: once a $V_S$ profile is obtained, it is possible to determine a dynamic G profile. In geotechnical engineering, the method commonly used to process the seismic signals is called SASW (Spectral Analysis of Surface Waves) (Stokoe *et al.*, 1994, Matthews *et al.*, 1996).

In this paper, we use SASW processing with the 3 sensors vertically polarized and located just below the sand surface plane (*Fig. 1*). In earth physics, more sophisticated signal processing techniques exist to extract information from surface waves (Abraham *et al.*, 1998). It requires a larger number of sensors but the experiment is easier and quicker. Furthermore, it avoids the following assumptions that will prevail in this paper :

- the signal is composed of surface waves only (noise from body waves is low),
- there is only one mode propagating (the first one).

Finally, due to the reduced number of sensors at our disposal for this study, we will assume that $V_S$ is constant with depth. Our aim is thus to find an average $V_S$ velocity value that, combined with an average $V_P$ velocity value, will lead to an approximate experimental value of the Poisson's ratio ν.

### Signal processing sequence.

The phase velocity $V_\varphi$ of surface waves is calculated with the phase φ of the cross spectral density of the signal of two consecutive sensors as follow:

$$V_\varphi = \frac{2\pi f d}{\varphi} \qquad (4)$$

where f is the frequency and d the distance between the two sensors. Tokimatsu *et al.* (1991) recommended the following rule (L is the distance between the source and the sensor nearest to it):

$$\frac{\lambda}{4} \le L \text{ and } \frac{\lambda}{16} \le d \le \lambda \qquad (5)$$

In our case, the wavelengths must be smaller than 36cm, the depth of the container. As the distance d equals either 12cm or 24cm, the wavelengths must be larger than 12cm.

The calculated dispersion curves (Herman, 1986), with Vp from Iwasaki and Tatsuoka's model and $\nu = 0.25$, show that the phase velocity between 0.9 to 1.9 kHz decreases less than 30 m/s. The constant Vs velocity profile assumption is thus acceptable with regard to preliminary surface waves study.

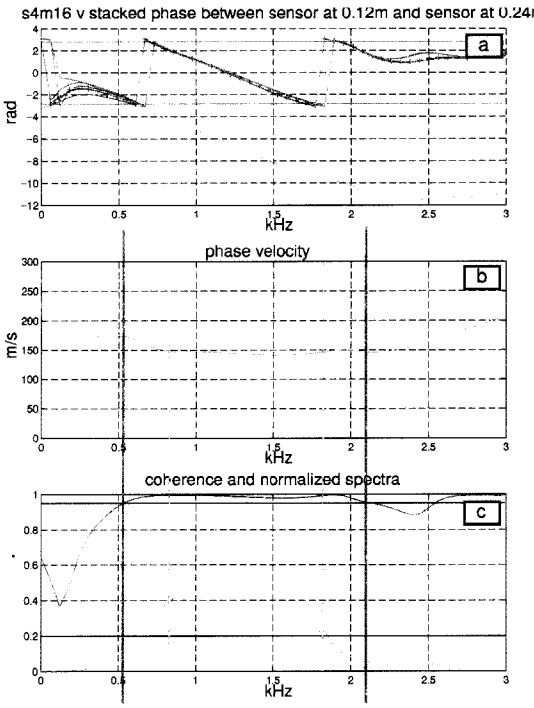


*Fig. 5. Phase velocity calculation*

For one couple of sensors, we first stack the phase of the 5 trials at our disposal (Fig. 5a), then we unwrap the phase sum (Fig. 5a) and finally calculate the phase velocity (Fig. 5b) with equation 4. We keep the value $V_\varphi$ when the coherence is higher than 0.95 and the amplitude of the normalized amplitude spectrum of each sensor is higher than 0.2 (Fig. 5c).

Results and discussion.

For each container, the sensor locations are the same and the phase velocity of all couples and foundation types are automatically calculated as above: their mean value for each acceleration level and each container is given in Table 2. Those values are given with a tolerance of ± 20m/s.

Table 2. Summary of measured $V_\varphi$, Vs and $\nu$

| | Container 1 | | | | Container 2 | | | |
|---|---|---|---|---|---|---|---|---|
| gravity g | $V_\varphi$ (m/s) | $V_P$ (m/s) | Vs (m/s) | $\nu$ | $V_\varphi$ (m/s) | $V_P$ (m/s) | Vs (m/s) | $\nu$ |
| 30 | ∅ | 283 | ∅ | ∅ | 133 | 271 | 164 | 0.29 |
| 40 | 165 | 299 | 181 | 0.21 | 144 | 287 | 155 | 0.29 |
| 50 | 176 | 313 | 193 | 0.19 | 152 | 300 | 143 | 0.30 |

Even though the standard deviation on measured velocity is high, their mean values show that the velocity slightly increases with the acceleration level. In the case of an homogeneous and isotropic elastic half space, the relation between $V_\varphi$, $V_P$ and $V_S$ is given by (Ewing *et al.*, 1957):

$$4\left[1-\frac{V_\varphi^2}{V_S^2}\right]^{1/2}\left[1-\frac{V_\varphi^2}{V_P^2}\right]^{1/2}=\left[2-\frac{V_\varphi^2}{V_S^2}\right]^2 \qquad (6)$$

Equation 6 is solved for $V_S$ (en hence for $\nu$) with Vp calculated at mid depth (*i.e.* 2.5 cm) and the result given in the last columns of Table 2 for each container.

If accurate values of $V_\varphi$ as a function of frequency were available (more measuring points are required) equation 6 would be replaced by an inverse problem. Its solution will lead to a $V_S$ profile.

## NUMERICAL MODELING OF SEISMIC WAVE PROPAGATION

### Finite element model

A finite element modeling of the propagation in the container was carried out both to confirm some of the above findings and to give a new insight in the complexity of the wave field.

Semblat (2000) showed that, for the analysis of wave propagation by numerical means, higher order finite elements is a very interesting alternative to reduce the number of elements and limit numerical dispersion (see Bamberger *et al.*,1980, Ihlenburg *et al.*, 1995). In this numerical part, we considered 9-node quadrilateral quadratic finite elements. The finite element model has a regular space discretization and includes 2163 quadrilateral elements of length $\Delta h$=0.01m leading to an amount of 8847 nodes. Considering the previous results, the elastic mechanical characteristics are chosen as follows : P-wave velocity varies from 220m.s$^{-1}$ near the surface to 520m.s$^{-1}$ at the bottom of the container, Poisson's ratio is 0.25, constant with depth.

For the computations, a vertical force was applied on the foundation corresponding to the one measured during centrifuge tests. The time step was $\Delta t$= 2.10$^{-6}$s. In this study, there is no algorithmic damping since we use a non dissipative Newmark time integration scheme (Hughes, 1987). The computations are performed thanks to the finite element code CESAR-LCPC (Humbert, 1989).

Wave propagation along the soil surface

In figure 6, horizontal displacements along the surface are plotted at different times. Considering these numerical results, two main waves types can be identified: P-wave from the faster small positive peaks and Rayleigh waves from the slower large peaks. The distance between both progressively increases with time. The hypothesis used in the shear waves section concerning the domination of Rayleigh waves is thus justified.

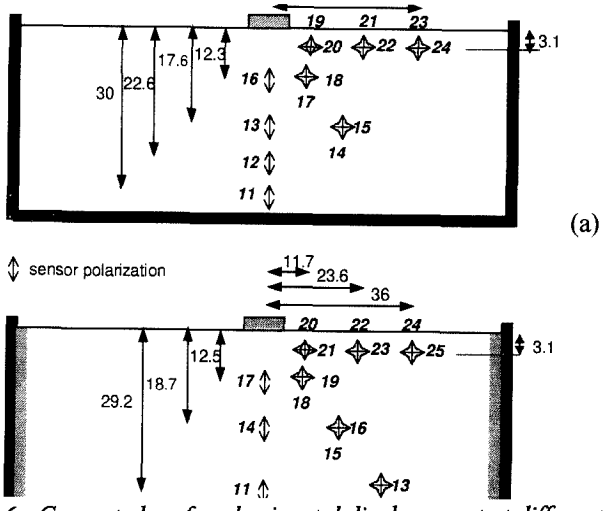


*Figure 6 : Computed surface horizontal displacement at different times.*

Wave characterization at « diagonal » sensors locations

At diagonal sensors locations (#17/18 and 14/15), horizontal and vertical computed displacements are plotted together. Figure 7 gives the corresponding curves with time as a parameter. For sensor 17/18 location, the displacement is purely diagonal at the beginning (1) showing the propagation of a pure P-wave. Afterwards (2), the displacement is transversal evolving in a wide loop influenced by both S- and Rayleigh waves. Further away from the source, at sensors 14/15 location, the effect of Rayleigh waves is much lower. The displacement is nearly diagonal (3) since sensors 14/15 are not exactly along the diagonal. Later, it is mainly transversal with a small loop showing some influence of Rayleigh waves (4). At both locations, P-waves appear clearly through peaks (1) and (3). For the two corresponding depths, the importance of Rayleigh waves is very different.

Figure 8 presents the same data but this time from real measurements. Of course, the aspect is not strictly the same but considering that they were obtained by double integration of acceleration data from embedded sensors, we find it of interesting similarity, validating the numerical description.

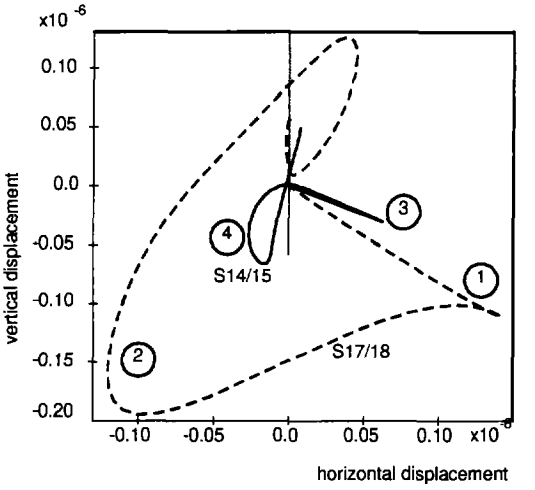


*Figure 7 : Vertical versus horizontal displacement for sensors locations #17/18 and 14/15 in container #1.(numerical)*

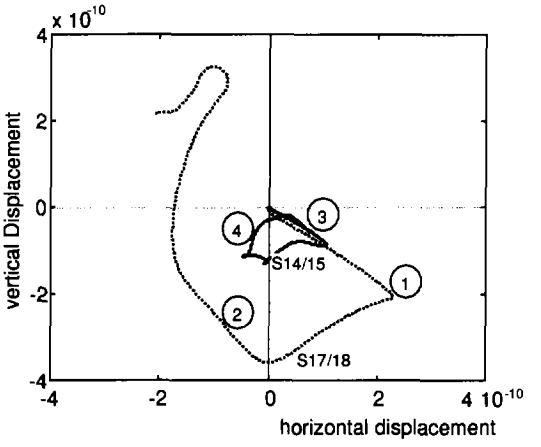


*Figure 8 : Vertical versus horizontal displacement for sensors #17/18 and 14/15 in container #1.(measured)*

Characterization in the whole container

To analyze seismic wave propagation in the whole container, displacements magnitude isovalues and displacement field vectors are plotted in figure 9 at time t = 0.012s. A faster P-wave appears clearly giving larger displacements along the vertical direction. At time t = 0.012s, it has already began to be reflected at the bottom of the container. After the P-wave front, other wave types take place. On the isovalue plot, one notices a large displacement area at the surface. As shown by the displacement vector plot, Rayleigh waves are mainly involved in this motion with a clear elliptic prograde movement. For the three types of sensors locations, the numerical results give different wave characterizations :

- surface locations : Rayleigh waves are mainly involved with a preliminary small P-wave peak,

- diagonal locations : pure P-waves appear clearly and Rayleigh waves are strong for shallow sensors and much smaller deeper in the container,
- vertical locations : pure P-waves are mainly involved.

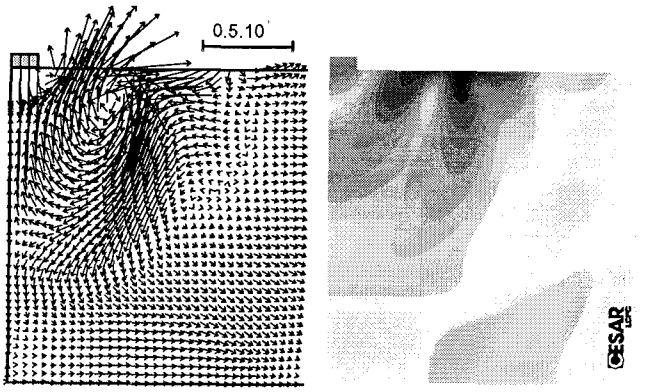


*Figure 9 : Isovalues of displacement magnitude and displacement field vectors at time t=0.012s.*

## CONCLUSION

This study confirms that wave velocities induced in a centrifuge container by vibrations of footings present a gradient with depth. A model based on Iwasaki and Tatsuoka's equation is consistent with propagation times of P-waves near the surface. Under the footing, this model is still valid but further experiments will be necessary to focus on the parameters of the model. A first evaluation of Vs and ν implementing SASW method validates Poisson's ratio 0.25 in these dynamic conditions. The FEM modeling confirms the above findings and contributes to the general conclusion that the field of waves is conform to what could be expected at prototype scale. These results concern short term behavior, before reflections occur. Further works will deal with long term behavior and damping.

## BIBLIOGRAPHY


Abraham O., H. Pedersen, Ph. Côte [1998]. *Determination of shear velocity profiles for soils and concrete by analysis of seismic surface waves.* In Proc. IV Meeting of the EEGS (European Section), Barcelona, Spain, pp395-398.

Bamberger A., G. Chavent, P. Lailly [1980], *Analysis of numerical schemes for linear elastodynamics equations* (in french), Report No.41, INRIA.

Coe, J, J.H. Prevost, R.H Scanlan [1985]. *Dynamic stress wave reflections/attenuation : earthquake simulation in centrifuge soil model*, Erthq. Engrg. and Struct. Dyn., Vol 13, pp 109-128.

Ewing W.M., W.S. Jardetzky, F. Press [1957]. *Elastic waves in layered media.* McGraw-Hill Book Company.

Hardin, B.O., V.P. Drnevich , [1972], *Shear modulus and damping ratio in soils: design equations and curves*, Proceedings ASCE, 98(7), pp 667-692.

Herman, R [1986], *Computers programs in sismology*, St Louis University, MO, USA.

Hughes T.J.R. [1987] *Linear static and dynamic finite element analysis*, Prentice-Hall, Englewood Cliffs, New Jersey.

Humbert P. [1989], *CESAR-LCPC : A general finite element code* (in french), Bull. des Lab. des Ponts et Chaussées, 160 : 112-115.

Kita L., T. Shibata, A. Yashima, S.I. Kobayashi [1992], *Measurement of shear wave velocities of sand in a centrifuge*, Soil and Found., Vol. 32 (2), pp134-140.

Ihlenburg F.,I. Babuška [1995] *Dispersion analysis and error estimation of Galerkin finite element methods for the Helmholtz equation*, Int. J. for Num. Met. in Engrg., 38 : 3745-3774.

Iwasaki T., F.Tatsuoka [1977], *Effects of grain size and grading on dynamic shear moduli of sands*, Soils and Found., Vol 17 (3), pp 19-35.

Matthews M.C., V.S. Hopes , C.R.I. Clayton [1996]. *The use of surface waves in the determination of ground stiffness profiles.* In Proc. Instn Civ. Engrs Geotech. Engrg., Vol. 119, pp. 84-95.

Pak R.Y.S. and B.B. Guzina [1995]. *Dynamic characterization of vertically-loaded foundations on granular soils*, J. of Geotech. Engrg., Vol. 121 (3), pp. 274-286.

Semblat J.F., M.P. Luong [1998]. *Wave propagation through soils in centrifuge testing*, J. of Earthquake Engrg., 2(1) : 147-172.

Semblat J.F.,J.J. Brioist [2000] *Efficiency of higher order finite elements for the analysis of seismic wave propagation*, J. of Sound and Vib., 231(2) : 460-467.

Siemer, Th, H.L. Jessberger [1994], *Wave propagation and active vibration control in sand* , C.F. Leung, F.H. Lee, T.S Tan (eds), Centrifuge 1994, Singapore, 31/08-2/09, A.A. Balkema, Rotterdam, pp 307-312.

Stokoe K.H., S.G. Wright, J.A. Bay, J.M. Roesset [1994]. *Characterization of geotechnical sites by SASW method.* In Proc. XIII ICSMFE, New Delhi, India. Oxford & IBH Publishing Co. Pvt. Ltd, pp. 15-25.

Tokimatsu K., S. Kuwayana, S. Tamura, Y. Miyadera [1991]. $V_S$ *determination from steady state Rayleigh wave method.* In Soils and Fund., Vol. 31, N°2, pp. 153-163.